Design of Rigid Pavement for Oke- Omi Road, Ibadan, Nigeria

Folake O. Akintayo and Toyin D. Osasona
Department of Civil Engineering, University of Ibadan, Ibadan, Nigeria
folakintayo@ui.edu.ng | tosasona16@gmail.com

Received: 22-APR-2022; Reviewed: 21-MAY-2022; Accepted: 29-AUG-2022
https://doi.org/10.46792/fuoyejet.v7i3.837

ORIGINAL RESEARCH

Abstract- Rigid pavements are often preferred to flexible types due to their higher durability and ease of maintenance also to reduce early road failure and increase its longevity. This study redesigned a deteriorated segment of Oke-Omi flexible road pavement as a rigid pavement. The pavement thickness was derived using the American Association of State Highway and Transportation Officials (AASHTO) design method. A programme using a spreadsheet was developed to facilitate the design process. The sieve analysis result showed that the soil was poorly graded. The soil has a low plasticity index of 28.1% (liquid limit 46.2%, plastic limit 18.1%); the Maximum Dry Density and Optimum Moisture Content were 1999 g/cm^3 and 10.8% respectively. The California Bearing Ratio of the soil was 48.43% which shows that the subgrade strength was adequate. The computed Estimated Single Axle Load (ESAL) for both the base year and the projected year are 6.74x10^6 and 100x10^6 single axle respectively. The design process yielded the pavement thickness of 240 mm and 380 mm for the base year (2017) and projected year (2037) respectively. A rigid pavement of adequate thickness was designed for the deteriorated segment of the Oke-Omi Road.

Keywords- Rigid Pavement, Estimated Single Axle Load (ESAL), Subgrade Strength, and Subgrade

1 INTRODUCTION

Technically, rigid pavement refers to any concrete road surface. According to AASHTO, a rigid pavement is a pavement structure that transmits loads to the subgrade and consists of a single course of Portland cement concrete with good bending resistance. The main benefits of using concrete pavement are its durability and its capacity to maintain a shape. Ashlesha et al. (2017) indicated that the ultimate goal is to ensure that the generated stresses caused by wheel load are appropriately decreased due to rigidity and high tensile strength. Flexible pavement allows for substantial deformation under large loads, this means the road will bend when under stress (Zulufqar et al., 2017).

When under stress, rigid pavement will hold its shape; however, if the tension is too great, it will break. Thus, as a result, the load is spread over a large surface of the sub-grade and the whole of the structural capacity in a rigid pavement. Wheel load stresses can be transmitted to a larger area below by rigid pavements because of their strong flexural structure. In contrast to flexible pavement, which is laid on a prepared subgrade, they are either laid directly on the prepared subgrade or as a single layer of granular or stabilized material. A country or region's ability to realize its economic potential will be constrained or hampered by the absence of high-quality roads. The longevity of roads has been ascribed to some factors which including poor design.

*Corresponding Author

Section E- CIVIL ENGINEERING & RELATED SCIENCES
Can be cited as:
Akintayo F.O. and Osasona T.D. (2022): "Design of Rigid Pavement for Oke-Omi Road, Ibadan, Oyo State", *FUOYE Journal of Engineering and Technology* (FUOYEJET), 7(3), 382-388. http://doi.org/10.46792/fuoyejet.v7i3.837

To reduce early road failure, rigid pavement has been designed to increase road durability. As the rigid pavement thickness increased, the tension stress at the top of the base layer steadily increased as well, up to a thickness of 300 mm, but the compression stresses at the top and bottom layers remained constant. Furthermore, there was no change in tensile stresses at the bottom of the base layer as the concrete slab thickness increased (Ahmed et al., 2020).

Oke-Omi Road is a major failed asphaltic road along the Iwo expressway in the northern part of Ibadan metropolis, Oyo State, due to a poor drainage system. This research aims to determine the concrete pavement thickness sufficient for the Oke-Omi Road to carry the projected design Estimate Single Axle Load (ESAL) by conducting a traffic analysis of the Oke-Omi Road and determining the geotechnical engineering properties of the subgrade soil.

2 MATERIAL AND METHODS

2.1 PRELIMINARY SURVEY

The necessary information about the physical features around the study route was noted and recorded. On Oke-Omi Road, a pavement evaluation was done to ascertain the cause of the pavement deterioration. Information gathered in this physical survey was used to design and developed the best method of rigid pavement design to prevent future problems.

2.2 RECONNAISSANCE SURVEY

This type of field survey was used to provide a means of verification of conditions as determined from the preliminary survey. It was done to examine the general character of the area.

2.3 GEOTECHNICAL INVESTIGATION

The objective of geotechnical investigation for this design is to predict experimentally the subgrade performance of the given soil. The following tests were carried out on the collected soil samples: Sieve analysis, Atterberg and compaction test.

2.3.1 Sieve Analysis

This test was conducted on the fine aggregate by BS 812: Section 103.1 2002. A known-weight sample of dry soil was poured into the top sieve, the nest was closed, and the sieve was agitated until each particle had descended to a sieve with perforations too small to pass through, at which point the particles were collected. The total weight of all material larger than each sieve size was calculated and divided by the total sample weight to arrive at the percent retained for that sieve size, which was then subtracted from 100% to arrive at the percent passing that sieve size. All soil samples were subjected to the same technique.

2.3.2 Atterberg Limit Test (Liquid and Plastic Limits)

Both the liquid and the plastic limits tests were carried out in one laboratory session by A.S.T.M. designation D4318 for the liquid limit, and D424 for the plastic limit. The liquid limit and the plastic limit, which was calculated by subtracting the plastic limit from the transmitted liquid limit, were also used to determine the plasticity index.

$$LL - PL = PI \quad (1)$$

2.3.3 Compaction Test

The process of compaction is the removal of air spaces in the soil in order to densify it. The optimum moisture content (OMC) and maximum dry density (MDD) of the soil are determined using ASTM D698: 2012. The moisture-density curve's OMC values were used to produce soil samples for CBR testing.

2.3.4 California Bearing Ratio Test

The California Bearing Ratio Test (CBR Test) is a penetration test developed by the California State Highway Department (USA) to determine subgrade soil bearing capability for pavement design. According to ASTM D1883:2021, the test was performed on compacted soils in wet conditions, and the results were compared to the curves of a known standard to determine the subgrade soil's strength.

2.4 The Rigid Pavement Design Process

2.4.1 Traffic load (W_{18}) Determination Traffic Study

A traffic count was conducted for seven days in a row. The average daily traffic (ADT) is based on a seven-day average, whereas the annual average daily traffic (AADT) is based on a year's average (AADT). The traffic forecast forecasts traffic volumes over the duration of the road's design life. The weight and number of daily repetitions of trucks and commercial vehicles were included in the design, however motorbikes in the traffic stream were not. The number of trucks in the design table, given as "trucks per day per lane," specifies how many load repetitions are imposed on the pavement each day. Because it is an existing road, the design term was widely deemed to be 20 years.

2.4.2 ESAL (Estimate Single–axle load) Computation

Equation 2 below was used to calculate the future cumulative flow in million standard axles (msa) for cv class T.

$$T = 365 \times F \times Y \times G \times W \times P \times 106 \quad (2)$$

$$Design\ Traffic\ (T) = \sum T$$

where F = Flow of Traffic (AADF) for each traffic class at the opening, Y = Design Period (20years), G = Growth Factor (from Table 2), P = Percentage of vehicles in the heaviest loaded lane (Figure 3), W = Wear Factor for each traffic class (from Table 1).

Table 1. Wear factors for CV Classes and categories

Wear Factors	Maintenance, W_M	New, W_N
Buses & Coaches	2.6	3.9
2-axle rigid	0.4	0.6
3 -axle rigid	2.3	3.4
4-axle rigid	3.0	4.6
3 & 4- axle articulated	1.7	2.5
5-axle articulated	2.9	4.4
6 -articulated	3.7	5.6

Source: DRMB (2006)

Table 2. Extracted Growth Factors (G) values

Design Period (Years)	OGV1+PSV	OGV2
5	1.07	1.05
10	1.04	1.12
15	1.06	1.19
20	1.09	1.27
25	1.11	1.36
30	1.14	1.45
35	1.17	1.50
40	1.19	1.07

Source: NRFT (1997)

Table 3. Recommended level of Reliability

Functional Classification	Urban	Rural
Interstate & other freeways	85-99.9	80-99.9
Other principal arterials	80-99	75-95
Collectors	80-99	75-95
Local	50-80	50-80

Source: AASHTO (1993)

Table 4. Suggested Levels of Reliability for Various Functional Classifications

	Standard Deviation, S_o
Flexible pavements	0.40-0.50
Rigid pavements	0.30-0.40

Source: AASHTO (1993)

2.4.3 Reliability (R%)

As indicated in Table 3, this determined the levels of assurance that the pavement portion constructed using this approach will endure for the design period. The reliability factor FR is determined:

$$\log_{10} F_R = -Z_R\, S_o \quad (3)$$

http://doi.org/10.46792/fuoyejet.v7i3.837 http://journal.engineering.fuoye.edu.ng/

where Z_R = Standard normal variant for given reliability (R%). Overall standard deviation ranges have been determined for both flexible and rigid pavements (90%). Performance criteria (serviceability indexes): Pavement condition is assessed using a present serviceability index (PSI), which has a range of 5 (Perfect Condition) to 0 (Impossible to travel). Initial serviceability index (Po), also referred to PSI, and is thought to be the lowest level that can exist before resurfacing or re-construction is required (1.5). The variation between Po and Pt (Po -Pt) is serviceability loss (ΔPSI). The basis for pavement design is ΔPSI.

2.5 Materials Properties for Structural Design

The modulus of the subgrade soil is the relationship between the California bearing ratio and the modulus of subgrade reaction K. Concrete properties include Modulus of Elasticity (Ec) and Modulus of Rupture (S'c). S'c was calculated using equation 4 to get the concrete's 28-day flexural strength. The force required to bend a beam under 3 points of loading was measured using a flexural test. Three grade 25 concrete beam specimens measuring 540 mm x 160 mm x 230 mm were prepared and cured for a 28-day period. The specimens were laid out on the compressive testing machine's support span (720mm), and a prescribed amount of load was applied to the centre by the loading nose, causing three-point bending. The average of the flexural load was obtained from the specimens.

$$S'C = \frac{3PL}{2bd^2} \qquad (4)$$

S'c= modulus of rupture, Psi
P = breaking load, (100,000N)
L= distance between knife edge, (360mm)
d= average specimen width, (115mm)

Elasticity modulus, of concrete, was obtained in equation 5 from the result obtained in Modulus of rupture (S'c) from equation 4

$$E_c = 5700(S'c) \qquad (5)$$

Thickness Determination: All the design input information was required before the determination of design thickness. The thickness of the rigid pavement was obtained by these two methods:

a. Computer Programming (Microsoft Excel)

The design parameters were inputted in the computer with their values respectively, while the pavement thickness D was assumed initially. Iterations were performed until the left-hand side of the equation equates to the right-hand side of equation 6.

b. Design Charts for Rigid Pavement

The design information was traced with a meter rule on the design charts in figures 2 and 3 under the following procedure:

Design Chart 1 (Figure 1)

Step 1: A horizontal line was drawn from the Effective Modulus of Subgrade Reaction, K, (500ib/in3) curve to the Modulus of Elasticity, EC, (4.222x106 ib/in2) curve and to the end of the box.

Step 2: From the first TL to the Mean Concrete of Rupture, S'c (740psi), a line was drawn.

Step 3: Another line was also drawn from the first T_L joining the second T_L intersecting Load Transfer Coefficient, J,

Step 4: Line from the second T_L intersecting the Drainage Coefficient, C_d (1.0) to the match line (68)

Design Chart 2 (Figure 2)

Step 1: The first TL line was intersected by the line drawn connecting the reliability level of 90% and the overall standard deviation SO of 0.4.

Step 2: Line joining point T_L the ESAL (W_{18}) 6.74X 10^6 was extended upward to intersect the line of design slab thickness (D)

Step 3: A line was drawn from match line (68) from the design chart 1 in figure 2 to design serviceability loss (1.5) to join the overall standard deviation (0.4)

Step 4: A horizontal line was drawn from ESAL to join the line from design serviceability loss (ΔPSI) on the design slab thickness line (D).

Step 5: Appropriate slab thicknesses were obtained on the line at which step 4 meets the designed slab thickness line (D).

2.6 Design Information for Oke-Omi Road

Initial Serviceability index, P_i= 4.5
Terminal serviceability index, P_t= 3.0
ΔPSI= 1.5
ESAL on design lane during first year of operation, W_{18}= 6.74x 10^6
Mean concrete modulus of rupture S'c= 740psi
Elastic Modulus, E_c= 4,220,000PSI
Drainage Coefficient C_d= 1.0 (Table 5)
Standard deviation, S_o= 0.4 (Table 4)
Reliability, R= 0.90 (Z= -1.282) (Table 5)
Modulus of Subgrade, K= 5000pci (Figure 3)
Load transfer coefficient= 3.9 (Table 5)

$$log_{10} W_{18} = Z_R X S_o + 7.35X\, log_{10}\,(D+1) - 0.06 + \frac{\frac{\log\left(\frac{\Delta PSI}{4.5-1.5}\right)}{1+1.624X10^7}}{D+1}(4.22-0.32P)X log_{10}\left(\frac{S_{c''} X C_d\,(D^{0.75}-1.132}{215.63\,X3\,(D^{0.75}-\frac{18.42}{\frac{(E_c)^{0.25}}{k}}}\right) \qquad (6)$$

http://doi.org/10.46792/fuoyejet.v7i3.837 http://journal.engineering.fuoye.edu.ng/

Table 5. Definition of Drainage Quality

Quality of Drained	Percent of Time Pavement Structure is Exposed to Moisture Levels Approaching Saturation			
	Less than 1%	1 to 5%	5 to 25%	Greater than 25%
Excellent	1.40-1.35	1.35-1.30	1.30-1.20	1.20
Good	1.35-1.25	1.25-1.15	1.15-1.00	1.00
Fair	1.25-1.15	1.15-1.05	1.00-0.80	0.80
Poor	1.15-1.05	1.05-0.80	0.80-0.60	0.60
Very Poor	1.05-0.	95 0.95-0.75	0.75-0.40	0.40

Source: AASHTO (1993)

Table 6. Load Transfer Joint (J)

Type of Shoulder	Asphalt		Tied PCC	
Load Transfer Devices	Yes	No	Yes	No
JPCP & JRCP	3.2	3.8-4.4	2.5-3.1	3.6-4.2
CRCP	2.9-3.2	N/A	2.3-2.9	N/A

Source: AASHTO (1993)

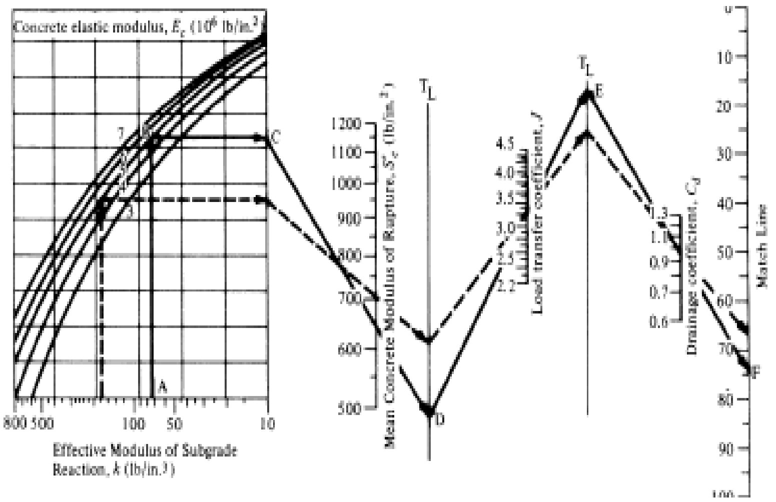

Fig. 1: Design Chart 1 for Rigid Pavements Based on Using Mean Values for Each Input

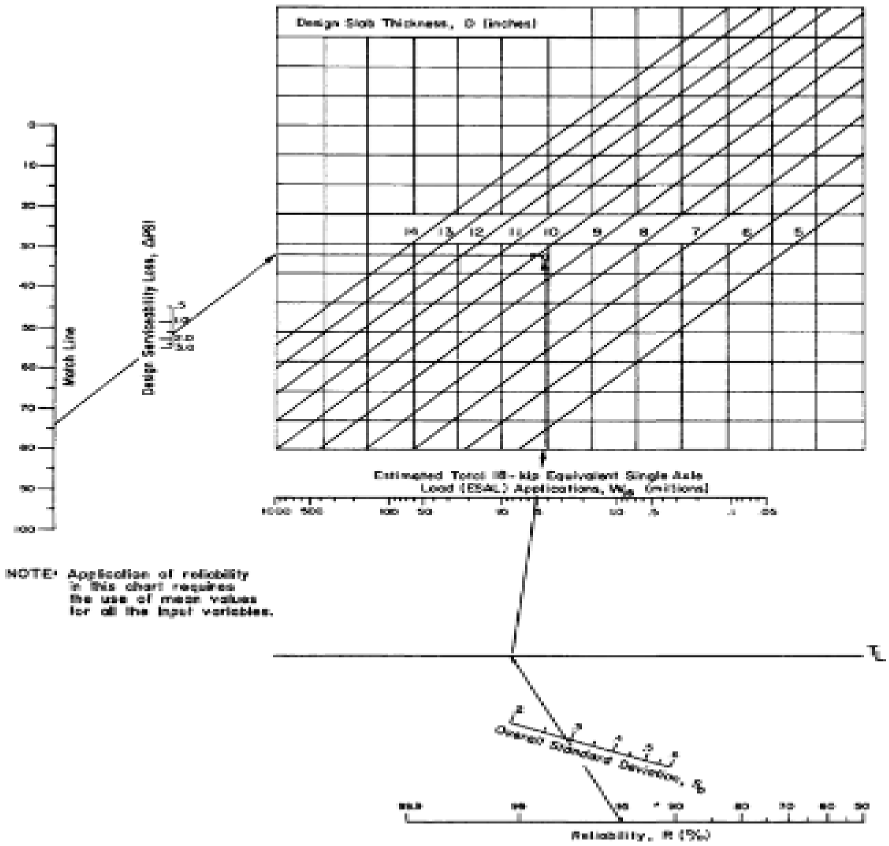

Fig. 2: Design Chart 2 for Rigid Pavements Based on Using Mean Values for Each Input

http://doi.org/10.46792/fuoyejet.v7i3.837 http://journal.engineering.fuoye.edu.ng/

3 Results and Discussion

3.1 Preliminary Survey

From the survey, it showed that Oke Omi road is an already existing deteriorated pavement due to impact from heavy wheel load.

3.2 Geotechnical Analysis

Two soil samples were collected from Oke-Omi road at intervals of 75 m at a depth of 1.0 m and were tested to determine the properties of the subgrade. The result showed that the two soil samples A and B are poorly-graded (GP). The AASHTO soil classification system showed that both soil samples fell within A-1-a. The absence of silt and clay from the result of the sieve analysis made the CBR to be high which is good for the subbase. According to the results of the Atterberg's limit test on the soil samples A and B, the liquid limits of the soil samples are 46.2 % and 46.5%. The plastic limits of the soil samples are 18.5% and 15% while the plasticity index of the soil samples is 28.1% and 31.5%, respectively which shows that the samples are less plastic. The modulus of subgrade reaction, which was determined from the CBR value, is 500 pci for the two compacted soil samples at optimal water content. The CBR value is high and it is, therefore, suitable for subbase. From the flexural strength result, the modulus rupture obtained is 740 psi and also elasticity modulus is 4,220,000 psi which is high enough to share the load over a large area of soil.

3.3 Traffic Volume Survey

The traffic volume survey was carried out along the study route for about a week. From the survey as presented in table 9, motorcycles and PSV (buses and coaches) had the highest percentage of road traffic. Considering the number of trucks exceeding 3tonnes, the road traffic is light. From the traffic volume survey chart while Estimated Single Axle Load (ESAL) computation is shown in the table 7. The annual designed traffic for the base year is 6.74 msa while the project designed traffic for 20 years is 100 msa.

3.4 Pavement Thickness

The pavement thickness was obtained from both computer programming (Microsoft Excel) and design charts (Figures 1 and 2). The result of the pavement thickness is 9.5 inches (240 mm) inches which is adequate for the study area considering the traffic volume in comparison with the existing literature. A prediction program was written using a spreadsheet with a ranging thickness from 180mm to 240mm were in the table 8. The program showed that 240 mm thickness was adequate using equation 5 for the year of design, while the thickness for 20 years of projection for the design traffic is 380 mm. The spreadsheet summary of the analysis is shown in table 10 below.

Table 7. ESAL Computation of Oke-Omi road

Commercial Vehicles	AADF (F)	Growth factor (G)	Wear factor (W)	Weighted annual traffic
Buses and Coaches	4593	1.09	2.6	5.06
2-axle rigid	1014	1.09	0.4	0.3
3-axle rigid	572	1.09	2.3	0.5
4 axle rigid	369	1.27	3.0	0.5
3 & 4 axle	210	1.27	1.7	0.2
5-axle articulated	76	1.27	2.9	0.1
6-axle articulated	44	1.27	3.7	0.05
Total	7978	Total weighted annual traffic		674 min
		% of vehicle heaviest lane(p)		74%
		Design period (Y)		20years
		Design traffic		100 msa

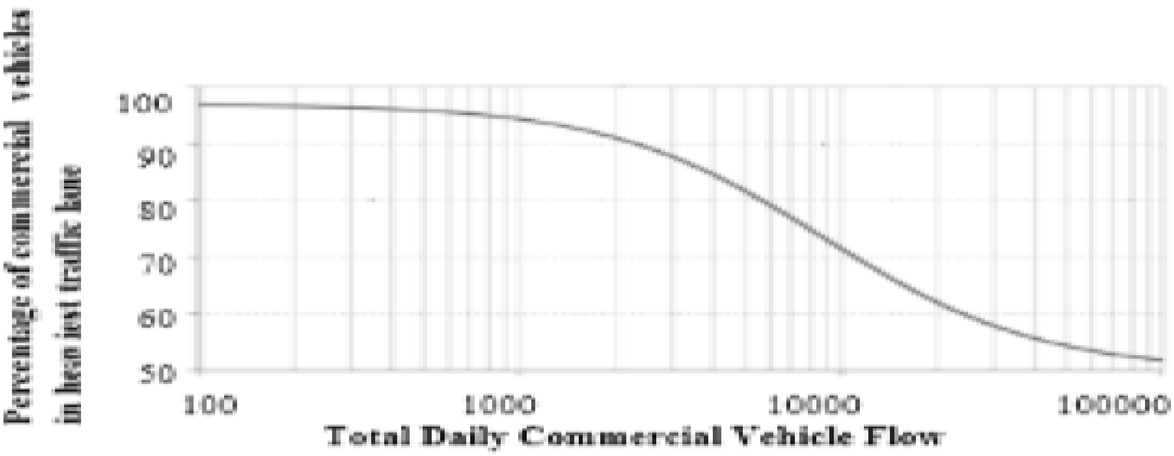

Fig 3: Percentage of Commercial Vehicles in Heaviest Loaded Lane (p); assumed depth (d) = 7 inches

http://doi.org/10.46792/fuoyejet.v7i3.837 http://journal.engineering.fuoye.edu.ng/

Table 8. Spreadsheet analysis for Trial 1 to 5

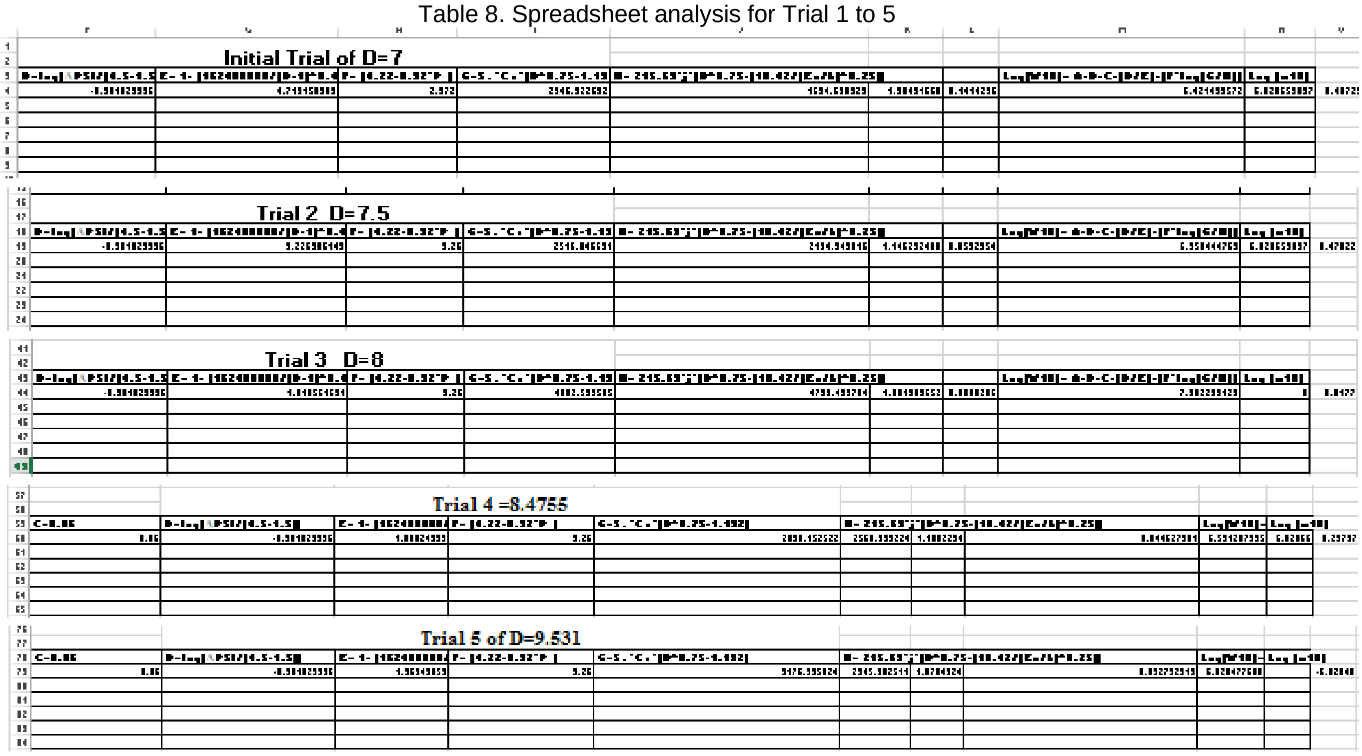

Table 9. Summary of the traffic volume survey

	Motor cycles	PSV, Buses &Coaches	OGV 1		OGV 2			
			2 axle rigid	3 axle rigid	3 axle articulated	4 axle rigid	5 axle articulated	6 or more articulated
Monday	1446	4550	1776	776	560	358	97	70
Tuesday	1883	3354	1500	510	488	200	80	54
Wednesday	1670	4400	1740	460	416	196	87	65
Thursday	1770	5100	1913	517	403	201	90	46
Friday	1188	6670	2210	678	333	250	88	35
Saturday	1170	5770	2330	620	277	164	78	26
Sunday	2002	4410	1230	440	105	102	15	14
Total	11129	34254	12699	4001	2582	1471	535	310
Average	1590	4893	1814	572	369	210	76	44
Percentage	17%	51%	19%	6%	4%	2%	0.8%	0.5%

Table 10: Summary of the Spreadsheet analysis

Thickness (mm)	Difference between Simulated ESAL & Actual ESAL
180	0.407200
190	0.470200
200	0.347100
220	0.234700
240	0.000200

Table 11. Engineering and Physical properties of Soil sample

Engineering and Physical Properties	Value
Liquid Limit (%)	46.2
Plastic Limit (%)	18.1
Plasticity Index (%)	28.1
Maximum Dry Density, MDD (g/cm³)	1999
Optimum Moisture Content (%)	10.8
California Bearing Ratio (%) Soaked	48.43
AASHTO Classification	A-1-a
USCS	GP

4 Conclusions

The absence of silt and clay materials from the result of sieve analysis of the subgrade soil makes the CBR value adequate for the sub-base soil. Also, existing traffic of Oke Omi road shows that buses are plying through the road than other vehicles. The pavement thickness obtained from both the design chart and spreadsheet analysis, using the CBR value and traffic volume values are the same (240mm). The major advantages of using concrete pavement are its durability and ability to maintain shape. It can be inferred from the existing literature that the rigid pavement's thickness is suitable for the design. (Garber and Hoel, 2009)

5 Recommendations

For the construction and reconstruction of new rigid pavement, a 20- or 30-year design period is used. For rigid pavements, it is preferable to consider a 30-year design term. Other significant factors must be taken into consideration if a design time other than 10, 20, or 30 years is chosen. Additionally, there is a need to investigate the impacts of climatic factors on rigid pavement design.

References

Ahmed A, Salam W, Nakin S. (2020). Effect of Pavement Foundation Materials on Rigid Pavement Response. Materials Science and Engineering, 3rd International Conference on Engineering Sciences IOP Conf. Series 671

Abiola, O.S, Owolabi, A.O.; Odunfa, S.O.; Olusola, A. (2010). Investigation into causes of premature failure of highway pavements in Nigeria and remedies.

(AASHTO) (1993). Guide for Design of Pavement Structures. American Association of State Highway and Transportation Officials, Washington, DC.

American Concrete Institute (ACI). (2004). Guide for Concrete Floor and Slab Construction. ACI302.1R-04. ACI,

Farmington Hills, MI.

AASHO 1962. Interim Guide for the Design of Rigid Pavement Structure.

Arora, K.R. (2003). Soil Mechanics and Foundation Engineering. Standard Publishers and Distributors, Delhi.

Ashlesha D., Kalinga, A., Dhapekar R (2017) study of rigid pavements – review. International Journal of Civil Engineering and Technology (IJCIET) Volume 8, Issue 6, June 2017, pp. 147–152

ASTM D698-12: (2012). Standard Test Methods for Laboratory Compaction Characteristics of Soil Using Standard Effort

ASTM 1833-21: 2021. Standard Test Method for California Bearing Ratio (CBR) of Laboratory – Compacted Soils.

Beckemeyer, C. A., Khazanovich, L., and Yu, H. T. (2002). Determining the Amount of Built-in Curling in JPCP: A Case Study of Pennsylvania I-80. Transportation Research Board Annual Meeting. Washington, D.C.

BS-812-103-1: 2003. Testing Aggregates Particle Distribution.

Cojocaru, R., Pais, J.C., Andrei, R. and Budescu, M. (2013). Modeling of Airport Rigid Pavement. Advanced Materials Research. Vol.649: pp.254-257.

Darestani, M.Y., Nataatmadja and Thambiratnam, D.P. (2006). A Review of 2004 Austroads Rigid

Pavement Design. ARRB Conference Research into Practice, Canberra, Australia.

Federal Ministry of Works and Housing, Lagos, Nigeria (1972), "Nigerian Highway Design Manual

Part I (Design) and Part II (Maintenance)"

Fernando, E.G., J. Oh, and D. Ryu. (2007) Phase I of M-E PDG Program Implementation in Transportation Engineering Journal ASCE, Vol.98: No.1, pp.37-4

Florida. Research Report No. D04491/PR15281-1, Texas Transportation Institute, The Texas A&M University System, College Station, Tex.

Garber, N.J. and Hoel, L.A. (2009). Traffic and Highway Engineering, 3rd edition, Pacific Grove, CA: Brooks-Cole

Hadi, M.N.S. and Arfiadi (2001). Optimum Rigid Pavement Design by Genetic Algorithms, Computers and Structures. Vol.1, No.5

Maharaj, D.K. and Gill, S. (2014). Development of Design Chart for Rigid Pavement by Finite, Element Method. International Journal of Latest Research in Engineering and Computing Vol.2: Issue 2, March-April, pp.27-39.

Milind V., Kadam K. A. (2016). Comparative Study on Rigid and Flexible Pavement. IOSR Journal of Mechanical and Civil Engineering. Vol 13

Nicholas J. Garber Lester A. Hoel. (2009). Traffic and Highway Engineering. 4th ed. University of

Virginia: United State of America Chapter 20: 1075-1131.

TxDOT, 2006. Section 3 — Pavement Types, Pavement Design Guide, pp 6-11, Technical Note.

Wang, S.K., Sergious, M. and Cheung, Y.K. (1972). Advanced Analysis Westergaard, H. M. 1927. Analysis of Stresses in Concrete Pavements due to Variations of Temperature. Proceedings of Highway Research Board. Vol. 6. National Research Council. Washington D.C. pp. 201-217.

Westergaard, H. M. (1926). Stresses in Concrete Pavements Computed by Theoretical Analysis. Federal Highway Administration. Washington D.C.

Zulufqar B. R, Rakesh G. (2017) Study of Defects in Flexible Pavement and its Maintenance.

